# Cooperative Grain Boundary Sliding and Migration Process in Nanocrystalline Solids

S. V. Bobylev, N. F. Morozov, and I. A. Ovid'ko*

*Institute of Problems of Mechanical Engineering, Russian Academy of Sciences, Bolshoj 61, Vasilievskii Ostrov, St. Petersburg 199178, Russia*

(Received 1 April 2010; published 30 July 2010)

A new physical mechanism or mode of plastic deformation in nanocrystalline metals and ceramics is suggested and theoretically described. The mode represents the cooperative grain boundary (GB) sliding and stress-driven GB migration process. It is theoretically revealed that the new deformation mode is more energetically favorable than ''pure'' GB sliding and enhances the ductility of nanocrystalline solids in wide ranges of their structural parameters.

DOI: 10.1103/PhysRevLett.105.055504 PACS numbers: 62.25.−g, 61.72.Lk

Physical mechanisms or modes of plastic deformation and behavior of defects in various nanostructures represent the subjects of intensive research efforts motivated by interest from both fundamental science and technology; see, e.g., [1–14]. For instance, specific deformation modes [carried by grain boundaries (GBs)] operate in nanocrystalline (NC) solids and, together with conventional slip of lattice dislocations (nucleated at GBs or interphase boundaries [15–17]), cause their unique mechanical properties such as superior strength and hardness; see reviews in [11–13] and the book in [14]. However, most NC solids have low ductility that limits their practical utility [11–14]. At the same time, there are several examples of superstrong NC solids showing substantial tensile ductility at room temperature [14,18–20] or superplasticity at elevated temperatures [12,14]. The nature of the outstanding combination of superior strength and good ductility is under debate [11–14]. Its understanding needs identification of specific physical modes of plastic deformation and their operation, together with lattice dislocation slip, in ductile NC solids. One of specific deformation modes is GB sliding, which, in particular, dominates in NC solids showing superplasticity [12,14]. Nonaccommodated GB sliding in NC solids creates defects—dislocations and disclination dipoles—at triple junctions of GBs [21,22]. These defects are capable of initiating cracks, in which case a NC solid tends to exhibit brittle behavior [21,22]. In contrast, if GB sliding is effectively accommodated, NC solids show enhanced ductility and/or superplasticity [12,14,23]. In this case, GB-sliding-produced defects transform into defect configurations which do not initiate cracks. In the context discussed, there is large interest in identification of accommodation mechanisms of GB sliding in NC solids. It is commonly viewed that accommodation of GB sliding occurs through lattice dislocation emission from triple junctions, diffusion, and rotational deformation [12,14,23]. All these processes transform defects produced by GB sliding and thereby are treated as ''active'' accommodation mechanisms. Besides, GB sliding produces extra GB curvature, which drives local GB migration in NC solids [12,23,24]. However, the curvature-driven migration of GBs does not transform defects produced by GB sliding and thereby can be viewed as a ''passive'' accommodation mechanism. The main aim of this Letter is to suggest and theoretically describe a new physical deformation mode—the cooperative GB sliding and stress-driven GB migration (CGBSM) process—involving GB migration as an active accommodation mechanism for GB sliding in NC solids.

Let us consider both pure GB sliding and the CGBSM process in a two-dimensional section of a deformed NC solid (Fig. 1). Pure GB sliding occurs under the applied shear stress $\tau$ and transforms initial configuration I of GBs [Fig. 1(b)] into configuration II [Fig. 1(c)]. GB sliding is assumed to be accommodated, in part, by emission of lattice dislocations from triple junction [Fig. 1(c)]. Besides, following the theories in [21,22], GB sliding results in formation of a dipole of wedge disclinations $A$ and $C$ in configuration II [Fig. 1(c)]. In general, a wedge disclination at a GB represents a line defect dividing GB fragments with different tilt misorientation angles, whose difference is the disclination strength [25]. In the considered case [Fig. 1(c)], the disclinations are characterized by strengths $\pm\omega$, whose magnitude ($\omega$) is equal to the tilt misorientation of the GB $AB$ assumed to be a symmetric tilt boundary. The disclination dipole $AC$ has the arm (the distance between the disclinations) equal to the magnitude $x$ of the relative displacement of grains [Fig. 1(c)]. The disclination dipole $AC$ is a GB-sliding-produced defect whose stress field can initiate a crack [21,22] [Fig. 1(d)].

Another deformation mode effectively operating in NC solids is the stress-driven GB migration; see pioneering experimental observations [26,27] and review [12]. It is a fast athermal process which (in contrast to thermally activated, curvature-driven migration of GBs) creates defects [28]. We think that both GB sliding and stress-driven migration can simultaneously occur as a cooperative stress-driven process, in which case defects created by GB sliding are, in part, accommodated by defects created by GB migration. In this context, the CGBSM process serves as a special deformation mode enhanced compared to pure GB sliding in NC solids. This view is supported by both our theoretical analysis given below and numerous

 © 2010 The American Physical Society

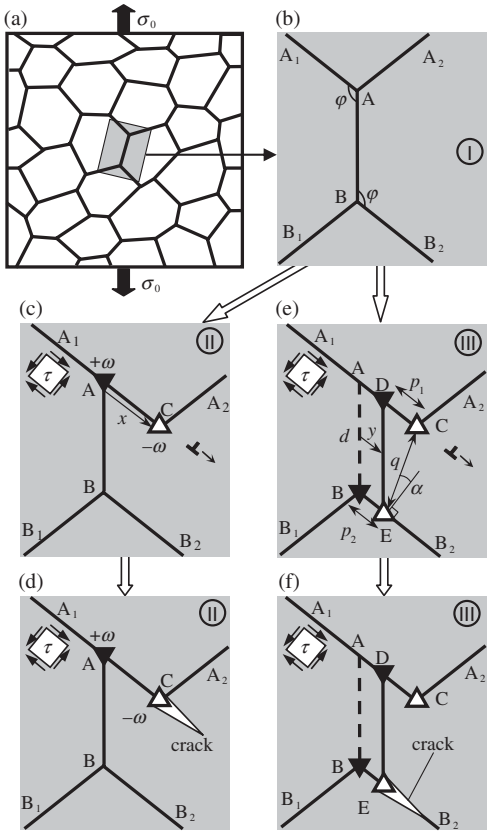


FIG. 1. Grain boundary deformation processes in nanocrystalline specimen: (a) General view. (b) Initial configuration I of grain boundaries. (c) Configuration II results from "pure" grain boundary sliding. Dipole of disclinations $AC$ is generated due to grain boundary sliding. (d) Crack forms and grows into the grain interior. (e) Configuration III results from cooperative grain boundary sliding and migration process. Two disclination dipoles $CD$ and $BE$ are generated due to this cooperative process. (f) Crack forms and grows along grain boundary fragment $EB_2$.

experimental observations [11,12,23,29] of concurrent GB sliding and grain growth occurring in NC solids during (super)plastic deformation.

Within our theoretical model, the CGBSM process transforms initial configuration I [Fig. 1(b)] into configuration III [Fig. 1(e)]. During this process, in parallel with GB sliding that causes the relative displacement of grains over the distance $x$, stress-driven migration of the vertical GB occurs over the distance $y$ from its initial position $AB$ to the new position $DE$ [Fig. 1(e)]. (Here, for simplicity, we consider GB configuration III with planar and parallel GBs $AA_1$ and $BB_2$, in which case the length of the migrating GB does not change. Examination of a more complex geometry is much more complicated and space-consuming, while its results are very similar with those of our simplified description.) Such a CGBSM process, in the spirit of the theories in [21,22,28], leads to the formation of two disclination dipoles $CD$ and $BE$ [Fig. 1(e)]. The dipole of wedge disclinations $CD$ is characterized by both the strength magnitude $\omega$ and the arm $p_1 = x - y$ (where $x \geq y$). The dipole of wedge disclinations $BE$ is characterized by both the strength magnitude $\omega$ and the arm $p_2 = y$. A crack may be formed in the stress field of a disclination dipole [Fig. 1(f)].

The transformation from the initial configuration (I) into the final configuration (III) is characterized by the change $\Delta W$ in the total energy of the solid. After some algebra in the spirit of the disclination theory [25], we find the following expression for the energy change:

$$\Delta W = \frac{G\omega^2}{4\pi(1-\nu)}\Big[p_1^2 \ln\frac{R}{p_1} + p_2^2 \ln\frac{R}{p_2} + L_1^2 \ln\frac{R}{L_1} + L_2^2 \ln\frac{R}{L_2} - L_{12}^2 \ln\frac{R}{L_{12}} - q^2 \ln\frac{R}{q} + \frac{(p_1+p_2)^2}{2}\Big] - \tau d(x + \omega y \sin\varphi). \quad (1)$$

Here $G$ denotes the shear modulus of the NC solid (assumed to be elastically isotropic), $\nu$ the Poisson's ratio, $q$ the distance between the disclinations $C$ and $E$, $\alpha$ the angle made by the segment $CE$ and the normal to the segment $BE$ [Fig. 1(e)], $R$ the screening length of the stress fields of disclination dipoles, $L_1 = \sqrt{p_1^2 + 2p_1 q \sin\alpha + q^2}$, $L_2 = \sqrt{p_2^2 - 2p_2 q \sin\alpha + q^2}$, and $L_{12} = \sqrt{(p_1 - p_2)^2 + 2(p_1 - p_2)q \sin\alpha + q^2}$. The first and second terms on the right-hand side of Eq. (1) characterize the elastic energy of the disclination dipoles (including the self-energies of both the dipoles and the energy of their interaction) and the work of the external stress $\tau$ spent to CGBSM process, respectively. The interaction of the disclination dipoles with other defects (say, other disclination dipoles produced by plastic deformation near the configuration shown in Fig. 1) leads to the mutual screening of their stresses. This effect is characterized by assigning a screening length $R$ to the stress fields of the disclination dipoles [21]. $R$ is approximately taken as a constant ($=3d$) for both the dipoles, because of low sensitivity of $\Delta W$ to $R$.

Equation (1) describes $\Delta W$ as a function of two variables $x$ and $y$. Figure 2 presents a typical map of the energy change $\Delta W(x, y)$, calculated by Eq. (1) within the intervals $x \leq d$ and $y \leq x$, for $R = 3d$, $\varphi = 2\pi/3$, $\tau = 0.01G$, $\nu = 0.34$, and $\omega = 0.3$. As it follows from Fig. 2, there is a minimum (shown as point $M_1$) at some values of $x_0$ and $y_0$. In doing so, the path $K$ from the starting point ($x = 0$, $y = 0$) towards the point $M_1$ is characterized by the absence of any energy barrier. That is, the process under consideration [Figs. 1(b) and 1(e)] is nonbarrier. Also, note that this CGBSM process is energetically preferred compared to pure GB sliding which corresponds to the path $S$ (Fig. 2) with a minimum of the energy change at point $M_2$. The preference is related to the definitive feature—cooperative character—of the CGBSM process. GB sliding and migration effectively accommodate each other when they simultaneously carry plastic flow [Fig. 1(e)], and this allows us to treat the CGBSM process as a special deformation mode

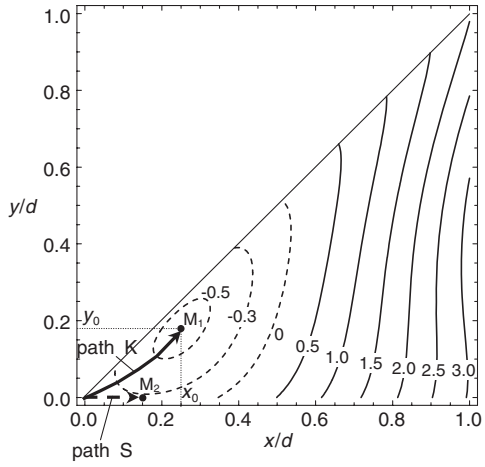


FIG. 2. Map of the energy change $\Delta W(x, y)$, calculated in the intervals of $x \leq d$ and $y \leq x$, for $R = 3d$, $\varphi = 2\pi/3$, $\tau = 0.01G$, $\nu = 0.34$, and $\omega = 0.3$. Values of $\Delta W$ are shown in units of $10^{-2}Gd^2/[2\pi(1-\nu)]$.

(different from either pure GB sliding or pure GB migration).

Dependences of parameters $x_0$ and $y_0$ on the disclination strength $\omega$ and the applied stress $\tau$ are presented in Figs. 3(a) and 3(b), respectively. Solid and dashed curves in Fig. 3(a) correspond to the dependences $x_0(\omega)$ and $y_0(\omega)$, respectively, calculated at various values of the normalized stress $\tau/G$. Solid and dashed curves in Fig. 3(b) correspond to the dependences $x_0(\tau)$ and $y_0(\tau)$, respectively, at various values of the strength $\omega$. Figure 3 shows that the CGBSM process is hampered when the disclination strength $\omega$ increases and enhances when the external stress $\tau$ grows. For instance, in a typical situation where the strength $\omega < 0.5$, the distances $x_0$ and $y_0$ may reach value of the grain size. When $\omega \sim 1$, the process is, in fact, suppressed (values of $x_0$ and $y_0$ are low).

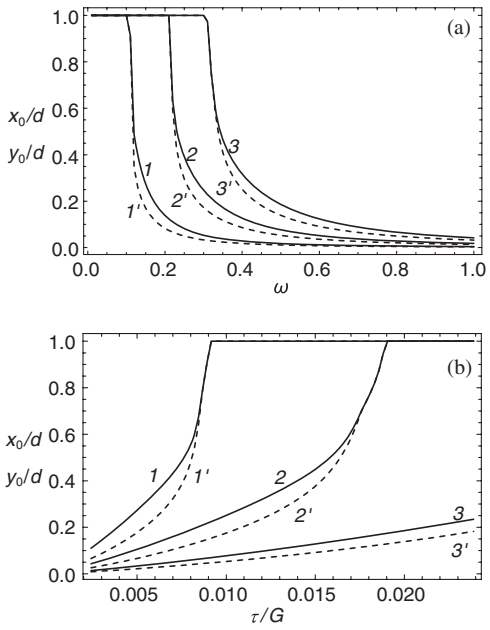


FIG. 3. Dependences of characteristics $x_0$ (solid curves 1, 2, and 3) and $y_0$ (dashed curves 1′, 2′, and 3′) on (a) the disclination strength $\omega$ [curves 1 (1′), 2 (2′), and 3 (3′) correspond to values of the normalized stress $\tau/G = 0.003$, 0.01, and 0.02, respectively] and (b) the applied stress $\tau$ [curves 1 (1′), 2 (2′), and 3 (3′) correspond to the disclination strength values of $\omega = 0.2$, 0.3, and 0.5, respectively].

The CGBSM process produces the local plastic strain $\varepsilon = \varepsilon_{\rm sl} + \varepsilon_{\rm mig}$, where $\varepsilon_{\rm sl}$ is the plastic strain carried by GB sliding and $\varepsilon_{\rm mig}$ is the plastic strain carried by GB migration. The plastic strain carried by GB sliding per one grain is given as $\varepsilon_{\rm sl} = x_0/d$ [21]. When pure stress-driven migration of a symmetric tilt boundary with misorientation $\omega$ occurs, it causes plastic strain $2\tan(\omega/2)$ within the area swept by the migrating GB. Since such an area normalized per grain area is approximately equal to $y_0/d$, the corresponding mean strain per one grain is $\varepsilon_{\rm mig} = 2y_0\tan(\omega/2)/d$. As a result, we find

$$\varepsilon = [x_0 + 2y_0\tan(\omega/2)]/d, \tag{2}$$

where the first and second terms describe plastic strains due to GB sliding and GB migration, respectively.

In recent years, particular attention has been paid to experimental results [18–20] giving evidence for enhanced tensile ductility of NC metals without preexistent cracks and pores, because these results are indicative of intrinsic ductility of NC structures. When a NC solid is free from fabrication-produced cracks, its tensile ductility is limited by plastic flow localization and/or brittle crack nucleation [11,14,22]. GB disclinations commonly cause pronounced strain hardening that suppresses plastic flow localization [22]. Therefore, in the considered case (Fig. 1), intrinsic ductility of a NC solid is controlled by crack nucleation. As a corollary, the ductility is approximately specified by the critical plastic strain $\varepsilon_c$ at which stable cracks nucleate in the solid. Let us estimate values of $\varepsilon_c$ in the cases of pure GB sliding and CGBSM process. To do so, we use the energy criterion [21] for crack nucleation and growth. According to this criterion, the formation of a stable crack with the length $l$ at a disclination dipole with the arm $p$ is energetically favorable, if $q(\tilde{l}) > q_c$. Here $\tilde{l} = l/p$,

$$q(\tilde{l}) = \tilde{l}\left[\left(\frac{2(\sqrt{1+\tilde{l}}-1)}{\tilde{l}} - \ln\frac{\sqrt{1+\tilde{l}}+1}{\sqrt{1+\tilde{l}}-1}\right)^2 + \left(\frac{2\pi(1-\nu)\tau}{G\omega}\right)^2\right], \tag{3}$$

the parameter $q_c = 32\pi(1-\nu)\gamma/(Gp\omega^2)$ when a crack nucleates or grows within a grain interior [Fig. 1(d)] or $q_c = 16\pi(1-\nu)(2\gamma - \gamma_b)/(Gp\omega^2)$ when a crack nucleates or grows along a GB [Fig. 1(f)], $\gamma$ is the specific free surface energy (per unit area), and $\gamma_b$ is the specific GB energy (per unit GB area) released when a crack nucleates or grows along the GB. As it follows from Fig. 1(d), in the case of pure GB sliding, the crack nucleates or grows

within the grain interior. In the case of CGBSM process, our calculations show that the dipole $BE$ in configuration III typically has a larger arm than the dipole $CD$ ($p_2 > p_1$) [Fig. 1(e)]. A dipole with a larger arm is a preferable site for crack nucleation. Besides, crack growth more easily occurs along GB (due to additional release of the GB surface energy) than within grain interior. As a corollary, a crack is typically generated near the disclination dipole $BE$, and its growth occurs along the GB fragment $EB_2$ [Fig. 1(f)]. Therefore, in the case of the CGBSM process, we focus our study on crack growth along the GB.

In general, the criterion (3) reveals the interval, $l_1 < l < l_2$, of crack length values corresponding to energetically favorable nucleation and growth of the crack. That is, any crack having its length $l$ within the interval grows until $l$ reaches value of $l_2$, in which case the crack becomes stable [21,22,28]. With the above formulas, we calculated local plastic strain $\varepsilon_c$, at which a stable crack with the length $l =$ 3 nm is formed in a NC nickel. In our calculation, we used $d = 30$ nm and $\omega = 0.5$ and 0.7 as parameters of the GB configuration, while we took the Ni material parameters as [30] $G = 73$ GPa, $\nu = 0.34$, $\gamma = 1.725$ J/m$^2$, and $\gamma_b = 0.69$ J/m$^2$. For these values, in the case of the CGBSM process [Fig. 1(f)], we found the equilibrium distances $x_0 \approx 0.22d$ and $y_0 \approx 0.17d$ at $\omega = 0.5$, as well as $x_0 \approx 0.12d$ and $y_0 \approx 0.10d$ at $\omega = 0.7$. The local plastic strain has a value of $\varepsilon_c \approx 0.31$ at $\omega = 0.5$ and $\varepsilon_c \approx 0.19$ at $\omega = 0.7$. In the case of pure GB sliding [Fig. 1(d)], with results from Refs. [21,22], one finds $p \approx 0.22d$ and $\varepsilon_c \approx 0.22$ at $\omega = 0.5$, as well as $p \approx 0.11d$ and $\varepsilon_c \approx 0.11$ at $\omega = 0.7$. These estimates allow us to conclude that the CGBSM process is characterized by significantly larger values of $\varepsilon_c$ compared to those for pure GB sliding.

Thus, the CGBSM process represents a special (new) deformation mode in NC solids. This deformation mode is more energetically favorable than pure GB sliding in NC solids in wide ranges of their parameters. It is theoretically revealed that intrinsic ductility (specified by the critical plastic strain $\varepsilon_c$, at which a stable crack with the length $l =$ 3 nm is formed) of a NC solid enhances, if the CGBSM process dominates, compared to the situation with dominant GB sliding. Results of our theoretical model are in a good agreement with experimental observations [11,12,23,29] of concurrent occurrence of GB sliding and grain growth in deformed NC solids.

The work was supported by the Russian Academy of Sciences Program ''Fundamental studies in nanotechnologies and nanomaterials,'' the NSF Grant CMMI #0700272, the Russian Ministry of Science and Education Grant MK-1702.2010.1, and the RFBR Grant 08-01-00225-a.

*Corresponding author.
ovidko@nano.ipme.ru

[1] L. Lu, M. L. Sui, and K. Lu, Science **287**, 1463 (2000).
[2] I. A. Ovid'ko, Phys. Rev. Lett. **88**, 046103 (2002).
[3] D. Farkas, M. Willemann, and B. Hyde, Phys. Rev. Lett. **94**, 165502 (2005).
[4] J. C. M. Li, Phys. Rev. Lett. **96**, 215506 (2006).
[5] Z. W. Shan, J. M. K. Wiezorek, E. A. Stach, D. M. Follstaedt, J. A. Knapp, and S. X. Mao, Phys. Rev. Lett. **98**, 095502 (2007).
[6] S. P. Joshi and K. T. Ramesh, Phys. Rev. Lett. **101**, 025501 (2008).
[7] X. L. Wu and Y. T. Zhu, Phys. Rev. Lett. **101**, 025503 (2008).
[8] I. Zizak, N. Darowski, S. Klaumunzer, G. Schumacher, J. W. Gerlach, and W. Assmann, Phys. Rev. Lett. **101**, 065503 (2008).
[9] S. V. Bobylev and I. A. Ovid'ko, Phys. Rev. Lett. **103**, 135501 (2009).
[10] X. L. Wu, Y. T. Zhu, Y. G. Wei, and Q. Wei, Phys. Rev. Lett. **103**, 205504 (2009).
[11] M. Dao, L. Lu, R. J. Asaro, J. T. M. De Hosson, and E. Ma, Acta Mater. **55**, 4041 (2007).
[12] A. V. Sergueeva, N. A. Mara, and A. K. Mukherjee, J. Mater. Sci. **42**, 1433 (2007).
[13] C. S. Pande and K. P. Cooper, Prog. Mater. Sci. **54**, 689 (2009).
[14] C. C. Koch, I. A. Ovid'ko, S. Seal, and S. Veprek, *Structural Nanocrystalline Materials: Fundamentals and Applications* (Cambridge University Press, Cambridge, 2007).
[15] M. Janecek, F. Louchet, B. Doisneau-Cottignies, Y. Bréchet, and N. Guelton, Philos. Mag. A **80**, 1605 (2000).
[16] P. M. Derlet and H. Van Swygenhoven, Scr. Mater. **47**, 719 (2002).
[17] F. Louchet, J. Weiss, and T. Richeton, Phys. Rev. Lett. **97**, 075504 (2006).
[18] K. M. Youssef, R. O. Scattergood, K. L. Murty, J. A. Horton, and C. C. Koch, Appl. Phys. Lett. **87**, 091904 (2005).
[19] S. Cheng, E. Ma, Y. M. Wang, L. J. Kecskes, K. M. Youssef, C. C. Koch, U. P. Trociewitz, and K. Han, Acta Mater. **53**, 1521 (2005).
[20] K. M. Youssef, R. O. Scattergood, K. L. Murty, and C. C. Koch, Scr. Mater. **54**, 251 (2006).
[21] I. A. Ovid'ko and A. G. Sheinerman, Appl. Phys. Lett. **90**, 171927 (2007).
[22] I. A. Ovid'ko and A. G. Sheinerman, Acta Mater. **57**, 2217 (2009).
[23] A. V. Sergueeva, N. A. Mara, N. A. Krasilnikov, R. Z. Valiev, and A. K. Mukherjee, Philos. Mag. **86**, 5797 (2006).
[24] K. A. Padmanabham and H. Gleiter, Mater. Sci. Eng. A **381**, 28 (2004).
[25] M. Kleman and J. Friedel, Rev. Mod. Phys. **80**, 61 (2008).
[26] M. Jin, A. M. Minor, E. A. Stach, and J. W. Morris, Jr., Acta Mater. **52**, 5381 (2004).
[27] W. A. Soer, J. Th. M. De Hosson, A. M. Minor, J. W. Morris, Jr., and E. A. Stach, Acta Mater. **52**, 5783 (2004).
[28] I. A. Ovid'ko, A. G. Sheinerman, and E. C. Aifantis, Acta Mater. **56**, 2718 (2008).
[29] A. K. Mukherjee, Mater. Sci. Eng. A **322**, 1 (2002).
[30] C. J. Smithells and E. A. Brands, *Metals Reference Book* (Butterworth, London, 1976).